



Continuous electropolishing technique for long-length Hastelloy C-276 tape

Shan-Peng Hao, Yi Wang, Hong-Li Suo* , Qiang Jia, Min Liu, Lin Ma

Received: 17 April 2018/Revised: 30 May 2018/Accepted: 18 June 2018/Published online: 9 August 2018
© The Nonferrous Metals Society of China and Springer-Verlag GmbH Germany, part of Springer Nature 2018

Abstract Preparation of the second-generation high-temperature superconducting tape by ion beam-assisted deposition (IBAD) requires a flat metal substrate. In this work, the electrochemical polishing of long-length Hastelloy C-276 alloy was studied, and its process parameters, characterized roughness and other properties were investigated. A 10-meter-long Hastelloy C-276 alloy was prepared by electrochemical polishing. The following optimized processing parameters are obtained: temperature of 45 °C, current density of 0.439 A·cm⁻² and polishing time of 60 s. The average roughness value (R_a) of the surface is less than 5 nm (5 μm × 5 μm), which was characterized by atomic force microscopy. This value satisfies the requirements for the further preparation of transition-layer pair by the IBAD technology route.

Keywords Hastelloy C-276 alloy; Electrochemical polishing; Atomic force microscopy; Current density

1 Introduction

The second-generation high-temperature superconductor YBa₂Cu₃O₇ (YBCO) has become a hot topic of research due to its obvious anisotropy, high critical current density, high irreversible field and great prospective applications in the field of superconducting transmission and as a superconducting magnet [1–5]. There are two main technical routes for the preparation of coated conductor templates: rolling-assisted biaxially textured substrate (RABiTS) and

ion beam-assisted deposition (IBAD) [6–10]. IBAD involves an ion beam-assisted deposition of a transition layer with a biaxial texture on a non-textured metal substrate, and then the deposition of a YBCO superconducting layer [11–16]. The IBAD technology route often uses a nickel-based stainless steel metal substrate, with the Hastelloy C-276 alloy substrate being the most widely used [17–20]. The subsequent preparation of the transition layer for the IBAD technique requires a high degree of flatness for the surface of the Hastelloy C-276 alloy substrate: The average roughness value (R_a) must be less than 5 nm in the range of 5 μm × 5 μm [21–24]. The roughness of the commercially available Hastelloy C-276 alloy substrate arises from the rolling level, and it is difficult to meet the IBAD technique requirements to prepare a uniform and dense transition layer. Therefore, the development and preparation of a high-surface-quality alloy strip is an urgent problem to be solved.

There have been many studies on the short tape polishing of a Hastelloy alloy. The Lawrence Berkeley National Laboratory in the USA used a 0.05-μm Al₂O₃ particle mill to polish the Hastelloy C-276 alloy baseband [25], whose R_a was reduced by 20 nm; Los Alamos National Laboratory first studied the continuous electrochemical polishing of Hastelloy in 2003 and compared the difference between electrochemical polishing and mechanical polishing [26]. SuperPower in the USA built a continuous polishing system for the Hastelloy C-276 alloy baseband in 2008 [27]. Qu et al. [28] used phosphoric acid (85 vol%), glycerol (15 vol%) and additives to polish the metal tapes, which resulted in a R_a value of less than 9 nm. Jia et al. [29] and Wang et al. [30] studied a short tape of Hastelloy C-276 whose R_a was 2.3 nm, but there are only a few studies on long-length tape polishing.

S.-P. Hao, Y. Wang, H.-L. Suo*, Q. Jia, M. Liu, L. Ma
School of Materials Science and Engineering, Beijing University of Technology, Beijing 100022, China
e-mail: honglisuo163@sina.com

To further produce a long-length alloy substrate with a high-quality surface, the processing parameters were explored and optimized for electropolishing 10-meter-long Hastelloy C-276, including polishing temperature, polishing time and current density. At the same time, a continuous electrochemical polishing test line was designed to provide equipment support for the surface leveling of a long-length Hastelloy C-276 alloy base.

2 Experimental

A Hastelloy C-276 alloy strip with a width of 1 cm and thickness of 77 μm was used, and the initial R_a of the alloy was approximately 20 nm. A continuous electrochemical polishing system was built, as shown in Fig. 1, where the device performed the sequence of unwinding–ultrasonic rough washing–rinsing–electrolysis polishing–rinsing–neutralizing–rinsing–ultrasonic finishing–rinsing–hot-air drying–drying–winding. Ultrasonic rough washing was performed with a mixture of acetone and alcohol with a concentration of 3%. The polishing liquid was composed of sulfuric acid (10 vol%), phosphoric acid (80 vol%) and chromic acid (10 vol%). The neutralization solution was an Na_2CO_3 solution ($0.1 \text{ mol}\cdot\text{L}^{-1}$). In the process of long-length substrate polishing, the substrate walks in the polishing liquid in a non-contact manner, so rectification was used to ensure the current of the substrate surface. The polishing time was converted by the speed of tapes and the distance of the polishing bath.

The non-contact mode of atomic force microscope (AFM; ICON) was usually used to measure the R_a of the substrate surface, but the original AFM can only measure short samples and the sample stage can only accommodate samples of up to 20 cm. To measure the surface roughness of a kilometer Hastelloy C-276 alloy, the walking bands device was designed and installed on the original AFM. The speed of walking, the precision of the step and the time were controlled by a computer, which facilitated the measurement of the surface roughness of long-length samples. The AFM scanning range was $5 \mu\text{m} \times 5 \mu\text{m}$, and the final data were the averages of the measurements from

ten points. A PHI-700 nm Auger electron spectroscope (AES) was also used to test the surface elemental distribution; an X-ray diffractometer (D8 Advance, XRD) was used to test the surface phase, and an HXD-1000 digital microhardness tester was used to test the microhardness of Hastelloy C-276.

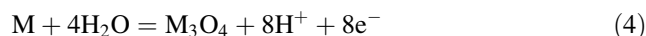
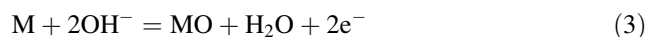
3 Results and discussion

3.1 Polishing principle

When the current density of the electrode is low, no electrochemical reaction occurs. When the current density further increases, the surface of the Hastelloy C-276 alloy begins to undergo a reaction. The metal atom loses electrons and becomes metal ions in the solution, as follows [31, 32]:



At a suitable value, a passivation film forms on the surface of the alloy, and a typical passivation reaction occurs. The metal atoms on the surface of the anode base substrate lose electrons and undergo oxidation reaction, resulting in a low-valence oxide:



At the same time, the oxides formed on the surface of the Hastelloy C-276 sample begin to become metal ions in the polishing solution, and the cathode surface begins to undergo a reduction reaction to generate oxygen:



The passivation layer in the protrusion is relatively thin and has a faster reaction rate at that point and is preferentially leveled and dissolved until a denser passivation layer is obtained, the metal substrate is gradually leveled, and the electrochemical polishing



Fig. 1 Photograph of electrochemical polishing system

effect is optimized. If the current density is too high, ultra-passivation will occur, resulting in a dense metal passivation film on the surface of the baseband, which will greatly increase the roughness of the surface of the baseband, so that the ultra-passivation stage will not achieve the effect of electrochemical polishing and leveling.

3.2 Temperature

The quality of an electrochemically polished surface depends on many factors, with temperature being the most important. Electrochemical polishing was performed at various temperatures from 10 to 70 °C, a fixed anode current density of $0.439 \text{ A}\cdot\text{cm}^{-2}$ and polishing time of 60 s, as shown in Fig. 2. When the polishing temperature is 10 °C, the Hastelloy C-276 alloy tape surface is relatively rough compared with the original surface (Fig. 3); no significant changes occur and the tape possesses a lot of the traces of rolling. When the polishing temperature increases to 30 °C, the traces of rolling gradually disappear. When the temperature is high (above 70 °C), the viscosity of the polishing liquid decreases, causing surface pitting corrosion.

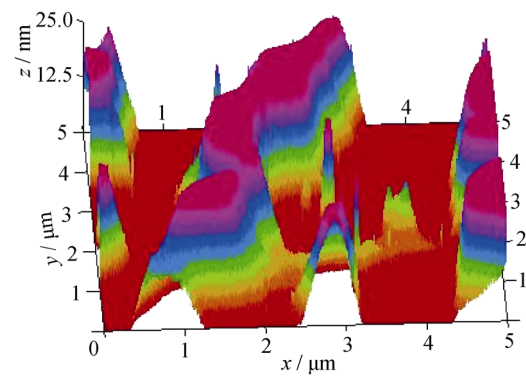


Fig. 3 3D AFM surface morphology of original Hastelloy C-276 alloy substrate

The temperature of the electrolyte was further adjusted to 30, 35, 40, 45 and 50 °C to study the effect of electrolyte temperature on the quality of the polishing. Figure 4 shows the AFM images of the three-dimensional morphology after electrochemical polishing at 30, 35, 40, 45 and 50 °C. When the electrolyte temperature is 30 °C, the electrochemical polishing temperature is too low and the polishing effect is limited; when the electrolyte temperature increases to 35 °C, the height of traces of rolling decreases; when the temperature of the electrolyte is 45 °C, most of the surface area is flattened and the original rolling marks

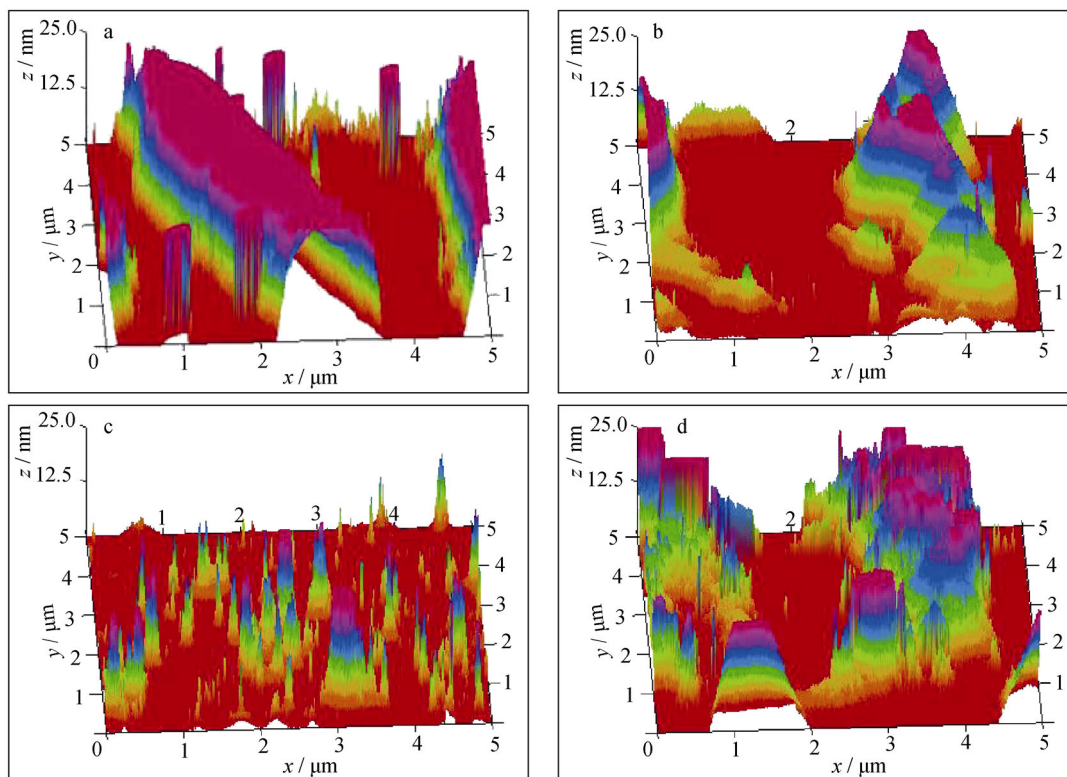


Fig. 2 3D AFM images of Hastelloy C-276 alloy substrate after electrochemical polishing at different electrolyte temperatures: **a** 10 °C, **b** 30 °C, **c** 50 °C and **d** 70 °C

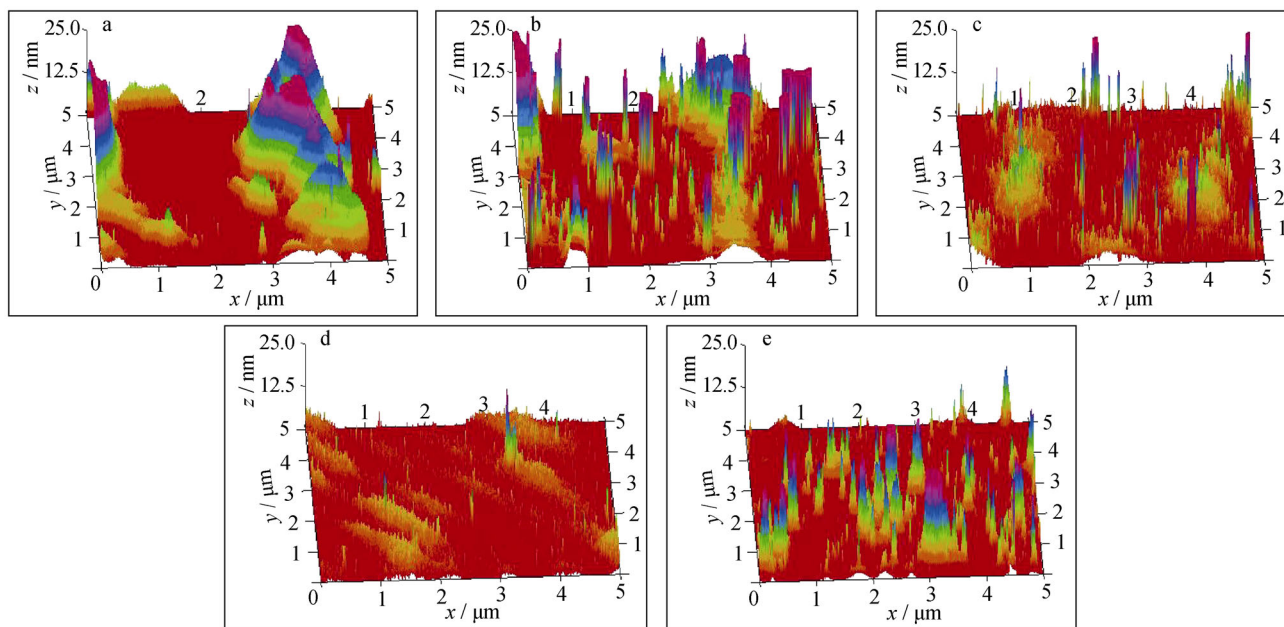


Fig. 4 3D AFM images of Hastelloy C-276 alloy substrate after electrochemical polishing at different electrolyte temperatures: **a** 30 °C, **b** 35 °C, **c** 40 °C, **d** 45 °C and **e** 50 °C

are only residual small bumps, compared with the original tape; when the temperature is 50 °C, the surface exhibits a slight corrosion and the distribution of the pits is uniform on the surface of the whole baseband.

Figure 5 shows the variation curve of R_a with the temperature of the electrolyte. The surface roughness shows a tendency to first decrease and then increase with the increase in temperature. When the temperature of the electrolyte is 45 °C, the R_a value of the surface of the Hastelloy alloy baseband is approximately 2.6 nm ($5 \mu\text{m} \times 5 \mu\text{m}$). With the further increase in temperature, R_a values increase correspondingly. When the temperature reaches 70 °C, the surface produces corrosive fringes which greatly increase the surface roughness of the

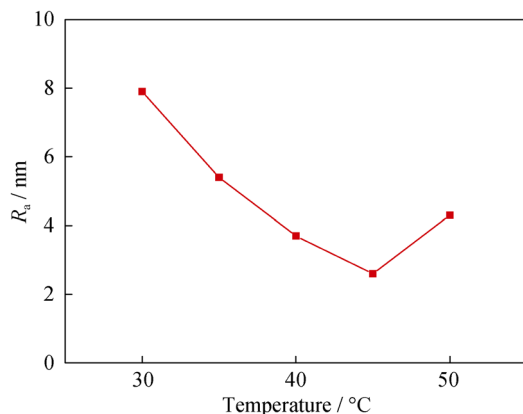


Fig. 5 Curve of surface roughness (R_a) changing at different electrolyte temperatures

baseband. As such, 45 °C is the ideal temperature to produce a metal alloy substrate with a high-quality smooth surface.

3.3 Anode current density and polishing time

Rectification was used to polish the long-length tape. The anode current density is a major factor affecting the polishing effect. The temperature of 40 °C and polishing time of 60 s were fixed. The anode current density was adjusted to 0.336, 0.388, 0.439, 0.491 and 0.543 $\text{A}\cdot\text{cm}^{-2}$. Figure 6 shows the three-dimensional AFM plots at different anode currents composed of AFM topography randomly taken from 10 points of the test. The rolling traces do not completely disappear when the current density is 0.336 $\text{A}\cdot\text{cm}^{-2}$. When the anode current density is 0.388 $\text{A}\cdot\text{cm}^{-2}$, the rolling traces of the baseband surface basically disappear and the residual part is slightly raised. When the anode current density is 0.439 $\text{A}\cdot\text{cm}^{-2}$, the surface of the baseband is super-flat and the surface is basically free from any defects with an R_a value of 2.4 nm ($5 \mu\text{m} \times 5 \mu\text{m}$), which meets the requirements of the IBA technology route. When the anode current density exceeds 0.491 $\text{A}\cdot\text{cm}^{-2}$, the baseband surface begins to produce pits. The sample of 0.543 $\text{A}\cdot\text{cm}^{-2}$ exhibits more pits than the 0.491 $\text{A}\cdot\text{cm}^{-2}$ sample, indicating that the polishing current is too high and the bubbles produced by the electrochemical reaction are unable to escape the liquid and cause the presence of pits.

As can be seen from Fig. 7, R_a also shows a tendency to first decrease and then increase with the current density

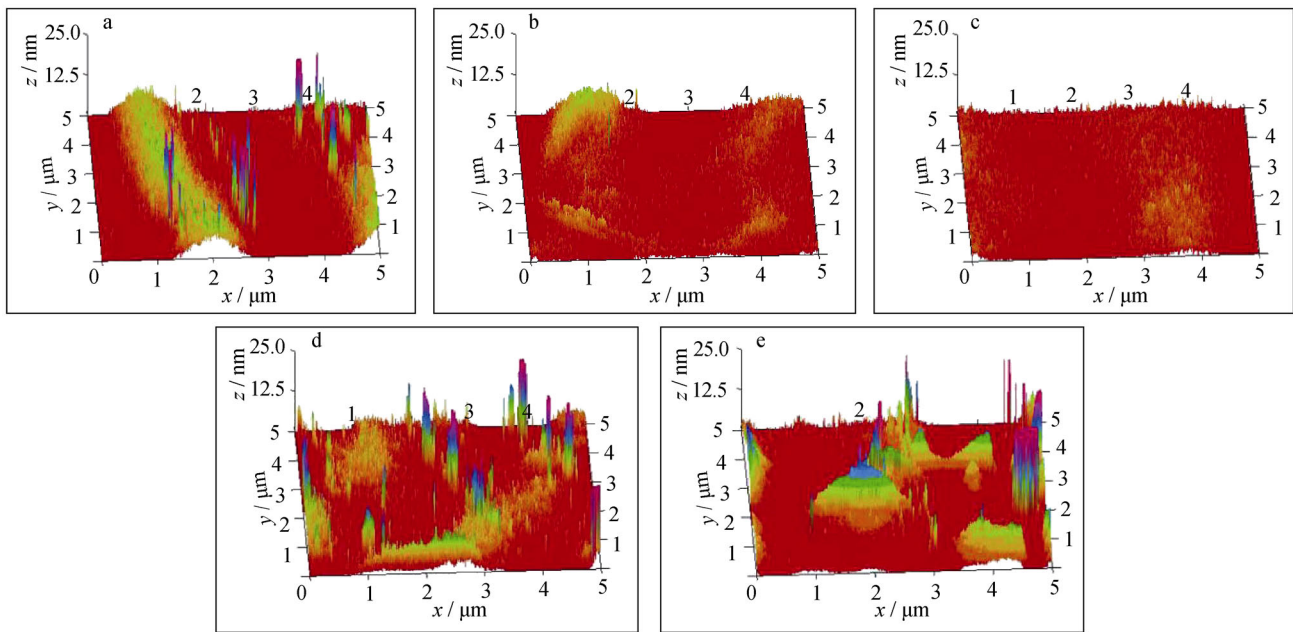


Fig. 6 3D AFM surface images with different anode current densities after electrochemical polish: **a** $0.336 \text{ A}\cdot\text{cm}^{-2}$, **b** $0.338 \text{ A}\cdot\text{cm}^{-2}$, **c** $0.439 \text{ A}\cdot\text{cm}^{-2}$, **d** $0.491 \text{ A}\cdot\text{cm}^{-2}$, and **e** $0.543 \text{ A}\cdot\text{cm}^{-2}$

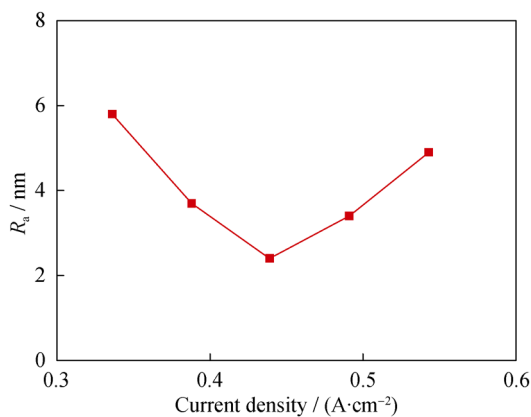


Fig. 7 Variation of R_a with different anode current densities after electrochemical polish

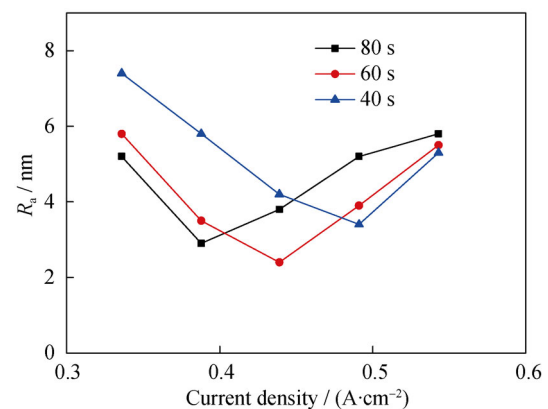


Fig. 8 Variation of R_a with different anode current densities and different polishing times

increasing. Taking into account the polishing effect and economic cost factors, the optimal anode current density is approximately $0.439 \text{ A}\cdot\text{cm}^{-2}$.

To study the polishing time, the electrochemical polishing temperature was fixed at 40°C , and the polishing time was varied (40, 60 and 80 s), where each polishing time corresponded to multiple sets of current densities. For a polishing time of 40 s, the surface roughness is much greater. With increasing polishing time, the surface roughness decreases. Polishing for 60 s produced a very smooth surface, with R_a value of 2.4 nm, as shown in Fig. 8. Polishing for longer time does not produce good results, so a suitable polishing time is 60 s.

3.4 Surface composition and XRD analysis

To understand the effect of electrochemical polishing on the surface composition of Hastelloy C-276 alloy, the surface elemental distribution of the alloy was analyzed by AES. Figure 9 shows the AES spectra of Hastelloy C-276, where the surface elements before and after polishing are basically similar, mainly including C, O, Ni, Cr, Fe and a small amount of N, P and other elements. After the polishing, the content of Ni in the metal is markedly reduced, and the chemical activities of Cr and Fe are similar and exhibit different degrees of precipitation. The original Ni alloy element with the largest content has the most reduction.

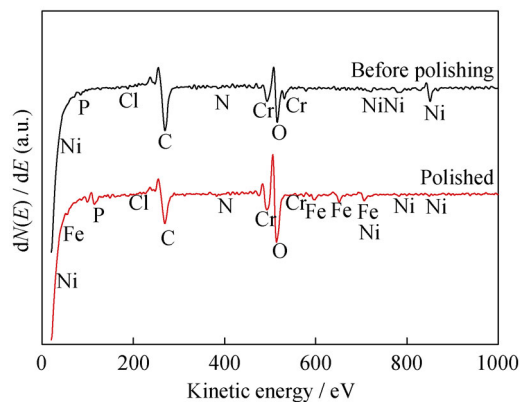


Fig. 9 AES patterns of Hastelloy C-276 before and after polishing, where $N(E)$ being Auger electron number and E being Auger electron energy

Before cleaning, the surface has some yellow material. This material could be dissolved in water and broke off easily after drying. XRD patterns in Fig. 10 show that the Hastelloy C-276 baseband is polycrystalline and exhibits three peaks between 10° and 80° , which are at 43° , 52° and 75° , respectively. Since the thickness of the film changes during the grinding process, the amount of Ni dissolved in the recess is very small, and under the action of the current, the selective dissolution of Ni occurs. In this step, Ni atoms are broken and move to the outside of the lattice. In the sulfuric acid and chromic acid phosphate dehydration, pyrophosphate is produced, Ni ions diffuse through the membrane to the surface, and the phosphoric acid reaction mainly produces $\text{Ni}_2\text{P}_2\text{O}_7$, as shown in Fig. 10. Phosphate dehydration formed pyrophosphoric acid, and Ni ions generated $\text{Ni}_2\text{P}_2\text{O}_7$. This process smooths the metal surface.

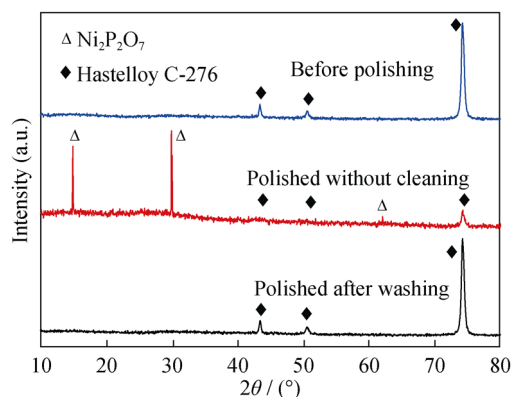


Fig. 10 XRD patterns of Hastelloy C-276 before polishing, polished without cleaning and polished after washing

3.5 Mechanical properties analysis

To explore the impact of electrochemical polishing on the mechanical properties of Hastelloy C-276, the HXD-1000 digital microhardness tester was used to test the microhardness of the Hastelloy alloy before and after polishing. As shown in Fig. 11, the hardness after polishing reduces by approximately 5% compared with that before polishing. The changes in the hardness of the Hastelloy C-276 before and after polishing are related to the changes in the surface-hardened layer. Electrochemical polishing eliminates the cold-work-hardened layer to some extent, which results in a decrease in alloy hardness.

3.6 Uniformity analysis

Based on previous results and discussion, the optimum process parameters are temperature of 45°C , anode current density of $0.439\text{ A}\cdot\text{cm}^{-2}$ and polishing time of 60 s. Then, the Hastelloy C-276 alloy baseband was polished in the polishing solution of the phosphoric acid–sulfuric acid–chromic acid system. The 10-meter-long Hastelloy C-276 alloy base was obtained and mounted on an AFM long band detection device to detect the surface roughness. A point was measured every 0.4 m, and its surface roughness value R_a was calculated using NanoScope 9X software. Figure 12 shows that the R_a value fluctuates up and down by 3 nm, it is stable, but there are jumping point fluctuations. The analysis results show that the surface roughness of the Hastelloy C-276 long band alloy baseband could effectively be reduced by continuous dynamic electrochemical polishing, which provides support for the industrialization of long baseband surface smoothing.

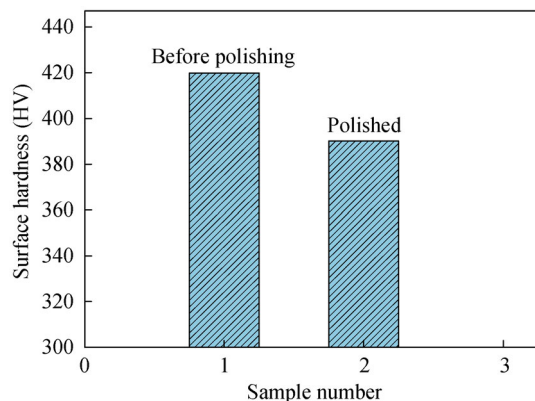


Fig. 11 Surface hardness of Hastelloy C-276 before and after polishing

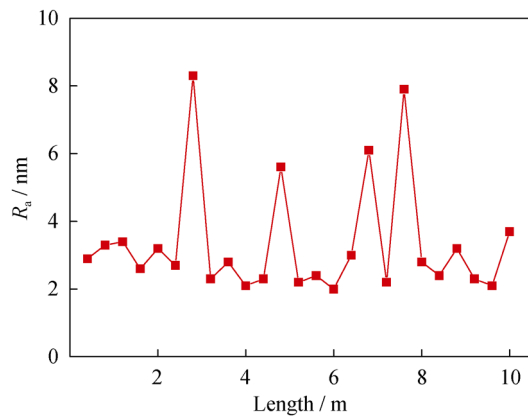


Fig. 12 R_a values for 10-m-long Hastelloy C-276 alloy substrates after electrochemical polish

4 Conclusion

An electrolysis solution of phosphoric acid and a phosphoric acid system were used to polish the Hastelloy C-276 alloy, and the Hastelloy C-276 alloy base with good effect was obtained. A suitable current density, the key parameter in electrochemical polishing, is found to be $0.439 \text{ A}\cdot\text{cm}^{-2}$. The other recommended electropolishing conditions are electrolyte temperature of $45 \text{ }^\circ\text{C}$ and time of 60 s. The influence of temperature and anode current density on surface roughness was intensively analyzed. After optimizing the optimal polishing parameters, the 10-meter-long Hastelloy C-276 alloy base was successfully prepared. After AFM test analysis, the average value of R_a is 3.4 nm and less than 5 nm ($5 \mu\text{m} \times 5 \mu\text{m}$), which satisfies the industrial demand for the preparation of superconducting materials by the technical route of IBAD.

Acknowledgements This study was financially supported by the National Science Foundation of China (Nos. 51571002, 51401003) and the Beijing Municipal Natural Science Foundation (Nos. 2172008, KZ201310005003).

References

- [1] Lu J, Abramov DV, Polyanskii AA, Gavrilin AV, Hilton DK, Markiewicz WD, Weijers HW. Field angular dependence of hysteresis losses of coated conductor for high field magnets. *IEEE Trans Appl Supercond.* 2013;23(3):8200804.
- [2] Kudymow A, Noe M, Schacherer C, Kinder H, Prusseit W. Investigation of YBCO coated conductor for application in resistive superconducting fault current limiters. *IEEE Trans Appl Supercond.* 2007;17(2):3499.
- [3] Yagi M, Mukoyama S, Amemiya N, Ishiyama A, Wang X, Aoki Y, Saito T, Ohkuma T, Maruyama O. Progress of 275 kV–3 kA YBCO HTS cable. *Physica C.* 2011;471(21):1274.
- [4] Wang P, Tian H, Suo HL, Ren C, Liang YR, Ma L, Liu M. Cube texture evolution of Ni_3W alloy substrates and La–Zr–O buffer layer of YBCO-coated conductors. *Rare Met.* 2016. <https://doi.org/10.1007/s12598-016-0790-8>.

- [5] Tian H, Suo HL, Wulff AC, Grivel JC, Mishin OV, Jensen DJ. Comparative characterization of CuNi substrates for coated conductors. *Alloys Compd.* 2014;601(601):9.
- [6] Kim KT, Lim JH, Kim JH, Joo J, Nah W, Ki BJ, Jun BH, Kim CJ, Hong GW. Development of cube-textured Ni–W alloy substrates for YBCO-coated conductor. *Physica C.* 2004;412–414(9):859.
- [7] Liu M, Meng Y, Zhao Y, Li FH, Gong YL, Feng L. Electropolishing parameters optimization for enhanced performance of nickel coating electroplated on mild steel. *Surf Coat Technol.* 2016;286:285.
- [8] Celentano G, Varesi E, Petrison T, Boffa V. Influence of the substrate microstructure on the superconducting properties of YBCO coated conductors. *IEEE Trans Appl Supercond.* 2003;13:2591.
- [9] Teranishi R, Izumi T, Shiohara Y. Highlights of coated conductor development in Japan. *Supercond Sci Technol.* 2006;19(3):S4.
- [10] Foltyn SR, Arendt PN, Dowden PC, Depaula RF, Groves JR, Coulter JY, Jia Q, Maley MP, Peterson DE. High T_c coated conductor-performance of meter-long YBCO/IBAD flexible tapes. *IEEE Trans Appl Supercond.* 1999;9(2):1519.
- [11] Goyal A, Ren SX, Specht ED, Kroeger DM, Feenstra R, Norton D, Paranthaman M, Lee DF, Christen DKM. Texture formation and grain boundary networks in rolling assisted biaxially textured substrates and in epitaxial YBCO films on such substrates. *Micron.* 1999;30(5):463.
- [12] Groves JR, Arendt PN, Foltyn SR, Jia QX. Improvement of IBAD MgO template layers on metallic substrates for YBCO HTS deposition. *IEEE Trans Appl Supercond.* 2003;13(2):2651.
- [13] Kaneko N, Iijima Y, Hanyu S, Sutoh Y, Kakimoto K, Saitoh T. Effect of substrate roughness on IBAD–GZO template layer. *Physica C (Amst, Neth).* 2006;445–448:445:608.
- [14] Kakimoto K, Sutoh Y, Ajimura S, Saitoh T, Iijima Y. Development of long Y-123 coated conductors by ion-beam-assisted-deposition and the pulsed-laser-deposition method. *Supercond Sci Technol.* 2004;17(5):S264.
- [15] Paranthaman MP, Aytug T, Stan L, Jia Q, Cantoni C, Wee SH. Chemical solution derived planarization layers for highly aligned IBAD–MgO templates. *Supercond Sci Technol.* 2014;27(27):1106.
- [16] Uprety KK, Ma B, Koritala RE, Fisher BL, Dorris SE, Balachandran U. Growth and properties of YBCO-coated conductors on biaxially textured MgO films prepared by inclined substrate deposition. *Supercond Sci Technol.* 2005;18(3):294.
- [17] Sarma VS, Boer BD, Reger N, Eickemeyer J, Opitz R, Holzappel B. Ni and Ni-alloy tapes with a very strong cube texture as substrates for high temperature superconducting tapes. *Mater Sci Forum.* 2002;408–412(11):1561.
- [18] Prusseit W, Nemetschek R, Hoffmann C, Sigl G, Lümke mann A, Kinder H. ISD process development for coated conductors. *Physica C.* 2005;426–431:866.
- [19] Chu JY, Zhao Y, Liu L, Wu W, Zhang Z, Hong Z, Li YJ, Jin ZJ. Topography evolution of rough-surface metallic substrates by solution deposition planarization method. *Appl Surf Sci.* 2018;427:237.
- [20] Sheehan C, Jung Y, Holesinger T, Feldmann DM, Edney C, Ihlefeld JF. Solution deposition planarization of long-length flexible substrates. *Appl Phys Lett.* 2011;98(7):169.
- [21] Fenga F, Shia K, Xiaoa SZ, Zhang YY, Zhao ZJ, Wang Z, Wei JJ, Han Z. Fractal analysis and atomic force microscopy measurements of surface roughness for Hastelloy C276 substrates and amorphous alumina buffer layers in coated conductors. *Appl Surf Sci.* 2012;258(8):3502.
- [22] Wang QY, Bai SL, Zhao YH, Liu ZD. Effect of mechanical polishing on corrosion behavior of Hastelloy C22 coating

- prepared by high power diode laser cladding. *Appl Surf Sci.* 2014;303(6):312.
- [23] Hu YN, Zhou H, Liao LP, Deng HB. Surface quality analysis of the electropolishing of cemented carbide. *J Mater Process Technol.* 2013;139(1):253.
- [24] Gaitzsch U, Jens H, Hühne R, Rodig C, Freudenberger J, Holzapfel B, Schultz L. High alloyed NiW substrates for low AC loss applications. *Supercond Sci Technol.* 2013;26(8):625.
- [25] Paranthaman MP, Aytug T, Stan L, Jia Q, Cantoni C, Wee SH. Chemical solution derived planarization layers for highly aligned IBAD–MgO templates. *Supercond Sci Technol.* 2014; 27(2):022002.
- [26] Kreiskott S, Arendt PN, Bronisz LE, Foltyn SR, Matias V. Continuous electropolishing of Hastelloy substrates for ion-beam assisted deposition of MgO. *Supercond Sci Technol.* 2003; 16(5):613.
- [27] Selvamanickam V, Chen Y, Xiong X, Xie Y, Zhang X, Rar A, Martchevskii M, Schmidt R, Lenseth K, Herrin J. Progress in second-generation HTS wire development and manufacturing. *IEEE Trans Appl Supercond.* 2009;19(3):3224.
- [28] Qu F, Liu HZ, Yang J, Gu HW. Electrochemical polishing of cubic texture Ni substrates for coated conductors. *Chin J Rare Met.* 2006;30(4):545.
- [29] Jia Q, Wang Y, Suo HL, Li MY. Electropolishing technique of Hastelloy C-276 alloy. *Rare Met.* 2017;36(8):635.
- [30] Wang Y, Wang P, Suo HL, Jia Q, Lu DQ, Li HZ, Wu HM. Electropolishing of Hastelloy C-276 alloy. *Mater Rev.* 2017; 31(2):37.
- [31] Wang X, Li CS, Yu ZM, Zheng HL, Ji YB, Fan ZG. Electropolishing process research of NiW alloy substrates. *Rare Met Mater Eng.* 2012;41(6):1075.
- [32] Feng F, Liu R, Chen H, Shi K, Wang Z, Wu W, Han Z. Substrate surface treatment and YSZ buffer layers by IBAD method for coated conductors. *Physica C.* 2009;469(15–20):1367.